International Journal of Mining Science and Technology 31 (2021) 103–110

Contents lists available at ScienceDirect

International Journal of Mining Science and Technology

journal homepage: www.elsevier.com/locate/ijmst

Assessing support alternatives for longwall gateroads subject to changing stress

Gabriel S. Esterhuizen [a,*], I. Berk Tulu [b], Dave F. Gearhart [a], Heather Dougherty [a], Mark Van Dyke [a]

[a] National Institute for Occupational Safety and Health, Pittsburgh Mining Research Division, Pittsburgh, PA 15236, USA
[b] West Virginia University, Morgantown, WV 26506, USA

ARTICLE INFO

Article history:
Received 10 July 2020
Received in revised form 1 September 2020
Available online 23 December 2020

Keywords:
Longwall
Gateroad
Support design
Coal
Standing support

ABSTRACT

Longwall gateroad entries are subject to changing horizontal and vertical stress induced by redistribution of loads around the extracted panel. The stress changes can result in significant deformation of the entries that may include roof sag, rib dilation, and floor heave. Mine operators install different types of supports to control the ground response and maintain safe access and ventilation of the longwall face. This paper describes recent research aimed at quantifying the effect of longwall-induced stress changes on ground stability and using the information to assess support alternatives. The research included monitoring of ground and support interaction at several operating longwall mines in the U.S., analysis and calibration of numerical models that adequately represent the bedded rock mass, and observation of the support systems and their response to changes in stress. The models were then used to investigate the impact of geology and stress conditions on ground deformation and support response for various depths of cover and geologic scenarios. The research results were summarized in two regression equations that can be used to estimate the likely roof deformation and height of roof yield due to longwall-induced stress changes. This information is then used to assess the ability of support systems to maintain the stability of the roof. The application of the method is demonstrated with a retrospective analysis of the support performance at an operating longwall mine that experienced a headgate roof fall. The method is shown to produce realistic estimates of gateroad entry stability and support performance, allowing alternative support systems to be assessed during the design and planning stage of longwall operations.

1. Introduction

Coal mines employing the retreat longwall mining method rely on gateroad entries to provide access and ventilation to the mining face. The entries are subject to changing horizontal and vertical stress as the longwall face approaches and mines by. The stress changes can cause significant roof, rib, and floor deformation requiring exceptional support measures. In the U.S., entry support in longwall gateroad entries typically consists of fully grouted solid bar bolts, partially grouted cable bolts, and various types of standing supports [1]. Coal ribs may be supported by various types of mechanically anchored bolts, grouted bolts, and screen [2]. Unfavorable combinations of stress and rock mass strength can result in roof instability that impacts safety, ventilation, and productivity.

Designing appropriate support for the variable geologic conditions and loading conditions typically encountered in a gateroad entry is challenging because of the large number of parameters that affect the stability of the excavation [3]. A successful ground control design is required to simultaneously consider the roof geologic composition, strength of individual roof beds, shear resistance of bedding planes, the initial vertical and horizontal stress magnitudes, the direction of the horizontal stress, longwall panel orientation, stress changes induced by the longwall extraction, rock mass response to these stress changes, and support alternatives to accommodate the roof deformation. Roof stability at the headgate T-junction is particularly challenging because the presence of the stage-loader and belt conveyor precludes the use of standing supports. Extreme support measures may be required in this area, such as a supplemental cable bolting and polyurethane injection into the roof strata [4].

At present, gateroad support systems are largely designed based on historical experience in similar geologic and operational settings. Standing support selection is facilitated by using the Support Technology Optimization Program (STOP) [5], which allows various commercially available standing support systems to be evaluated. However, gateroad roof falls remain a safety and productivity concern in modern, high-production longwall mines [6].

* Corresponding author.
E-mail address: eee5@cdc.gov (G.S. Esterhuizen).

https://doi.org/10.1016/j.ijmst.2020.12.016
2095-2686/

The National Institute for Occupational Safety and Health (NIOSH) has conducted research to address the need for a method of assessing longwall gateroad support alternatives. The research was conducted through a combined program of data collection on current gateroad support practices [1], testing of gateroad support systems [7], monitoring of longwall-induced ground deformation, stress changes, and support response at longwall operations in the U.S. [8–10], analysis of the results, and development of numerical modeling procedures [11–13] that allow expected support performance and ground stability under changing stress to be evaluated.

This paper describes how the developed numerical models were used to conduct parametric studies in which the important factors affecting entry stability under changing stress were evaluated. The results of the parametric studies were used to develop two regression equations that can be implemented in a spreadsheet-type analysis to assess likely ground deformation, support loading, and support performance in longwall gateroads. The outcome of the proposed assessment procedure is a roof stability rating (RSR) that allows different support alternatives to be compared for given mine layouts, geologic conditions, and longwall-induced loading conditions.

2. Parametric studies using numerical models

Monitoring rock mass response and support performance in the field is costly and time consuming. In this research, numerical models were used to supplement field data with information about support system performance under geologic and stress conditions beyond those that were measured in the field. The FLAC^{3D} V5.1 finite difference software package [14] was used to conduct the parametric studies. The modeling procedures used were originally developed to model support needs for coal mine entries under development conditions [15,16]. For the assessment of gateroad entries, the model boundaries were subject to gradually increasing loads to simulate the effect of an approaching longwall face [11]. The input parameters and modeling procedures were verified against gateroad monitoring results at operating mines to ensure that reasonable estimates of ground deformation and rock mass yield were achieved [10–12].

Fig. 1 shows an example of a typical numerical model result indicating rock mass damage, the resulting rock mass deformation, and support loading. The rock mass damage shown in Fig. 1a illustrates how several rock failure modes are captured by the models and how a dome of yielding rock is formed above the entry. Fig. 1b shows the same entry at a later stage of loading, where the cable bolts have failed, and the yielded roof rock is now resting on the standing supports. The load in the bolts and cable bolts is shown, as well as the stress within the standing supports.

2.1. Geologic scenarios evaluated

The parametric studies considered ten different geologic scenarios. Four of the scenarios were based on actual mine sites where field monitoring was conducted, and five were geological conditions that were selected to investigate specific geological settings. Table 1 lists the ten geological scenarios and the depth of cover ranges considered.

2.2. Depth of cover and horizontal stress scenarios

The numerical models were set to simulate depths of cover ranging from 182 to 609 m (600–2000 ft). Not all geologic scenarios were assessed at all depths of cover because the weaker roof cases collapsed under development conditions at the greater depths. The models were subject to a series of stress increments of 2.0 MPa (300 psi) each to simulate the effect of an approaching longwall panel. The stress increments were selected to provide horizontal-to-vertical stress increment ratios of between 0.33 and 3.00. For each analysis, the stress was increased until the roof sag in the model exceeded 0.30 m (12 in) or the applied stress increase exceeded 27.5 MPa (4000 psi).

2.3. Support systems evaluated

Support systems consisted of roof rock reinforcement by fully grouted bolts or fully grouted bolts and cable bolts. Supplemental support using various types of standing supports was also modeled. The roof reinforcement consisted of various combinations of 1.8- and 2.4-m-long (6- and 8-ft-long) fully grouted bolts with peak tensile strength of 20 t. Cable bolts with lengths of 3.0, 3.6, and 4.8 m (10, 12, and 16 ft) and maximum tensile strength of 30 t were modeled.

Standing supports were modeled as passive supports installed after the initial roof sag associated with entry development had occurred. Standing support loads were, therefore, generated by roof deformation caused by the approaching longwall face. The load-deformation curve for the standing supports was based on

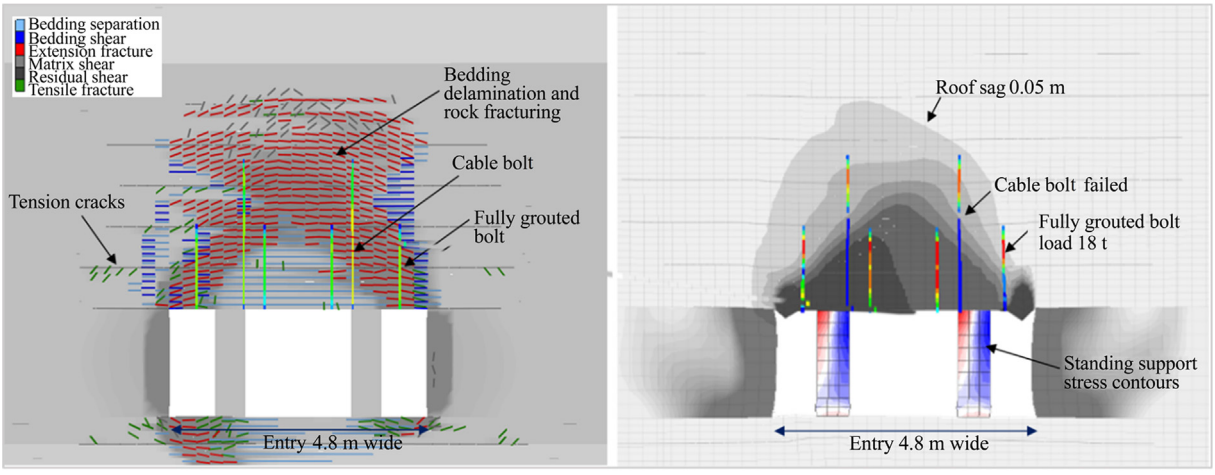

(a) Rock-failure modes (b) Roof deformation and support response

Fig. 1. Example of FLAC^{3D} numerical model results of entry and support response to longwall-induced loading.

Table 1
Geologic scenarios evaluated.

Description	Depth (m)
Kittanning coal bed	182, 243
Pittsburgh coal bed	228
Colorado D-seam	365
Pocahontas coal bed	609
Pittsburgh coal bed	243
Weak immediate roof test	182–304
Weak upper roof test	182–304
Uniform weak roof test	182–304
Moderate roof test	182–609
Strong roof test	182–609

testing results obtained at the NIOSH Mine Roof Simulator and presented in the STOP software. Support types evaluated included: 3.15-mm (9-pt) timber cribs, engineered timber cribs, engineered timber props, and cementitious yieldable cribs of various capacities. The supports modeled represent the typical range of standing support capacities currently used in U.S. longwall gateroads.

3. Procedure for assessing the RSR

The roof stability rating (RSR) was developed to rate the ability of the roof support system to control the yielded roof strata that would collapse if unsupported. Multi-parameter linear regression analyses and curve fitting techniques were used to explore the relationships between roof deformation, rock strength, loading conditions, and support performance determined through the parametric studies. The RSR is calculated by considering the impact of the roof sag on the support system, the height of yielded roof that may potentially collapse, and the support system capacity. The next sections describe how these parameters are estimated and how the RSR is calculated from the results.

3.1. Regression equation to estimate roof sag caused by longwall-induced stress changes

An equation to estimate the longwall-induced roof sag at the roof line was derived by multiple linear regression analysis of the parametric study results. The effects of the independent variables were initially assessed to establish which parameters have the most significant impact on roof sag. Parameters that were strongly correlated were combined to reduce interactions in the analysis, while parameters with limited impact on the roof sag were eliminated. Any variables that had p-values above 0.05 (indicating limited significance) were eliminated.

The final seven parameters selected for roof sag prediction were as follows, in descending order of importance: (1) longwall-induced horizontal stress, (2) initial horizontal stress in the entry roof, (3) field-scale strength of the roof strata within the fully grouted bolt horizon, (4) field-scale strength of the roof strata in the cable-bolt anchorage horizon, (5) longwall-induced vertical stress, (6) standing support capacity, and (7) reinforcement capacity (bolts and cable bolts). The regression equation to predict roof sag has a coefficient of determination (r^2) value of 0.78 with a root mean square error of 0.012 m (0.5 in).

The regression analysis showed, not unexpectedly, that the parameters that have the greatest impact on roof sag are related to the stress state and the roof strength, while the support system has a lesser effect. The limited impact of the support system on the longwall-induced roof sag can be explained by the fact that the equivalent pressure exerted by the support system distributed over the full width of the entry may be in the order of 0.20–0.27 MPa (30–40 psi), while the stress changes that are driving the roof yield can be as high as 6.89–13.78 MPa (1000–2000 psi), depending on depth of cover and distance from the longwall face. The support pressure is, therefore, about two orders of magnitude smaller than longwall-induced stress that drives the roof yield and associated dilation. In-mine monitoring has also shown that changes in standing support systems appear to have limited impact on roof deformations induced by longwall mining [17].

The equation to estimate the roof sag (s) at the roof line of a gateroad entry has three components.

$$s = (S1 + S2 + S3 + C)^2 \tag{1}$$

where S1 is the stress state; S2 the roof strength; S3 the support efficiency; and C a constant determined from the regression analysis. Each component may be calculated as follows.

$$S1 = 0.1345 \times Hinc + 0.0319 \times Vinc + 0.279 \times SIGHini \tag{2}$$

$$S2 = -0.117 \times ((RSa + 2 \times RSi)/3.0) - 0.0126 \times RSc \tag{3}$$

$$S3 = -0.0028 \times SSc - 0.0023 \times (RRb + RRc) \tag{4}$$

$$C = 1.237 \tag{5}$$

where *Hinc* is the horizontal stress increase induced by the longwall panel (MPa); *Vinc* the vertical stress increase (MPa) induced by the longwall panel; *SIGHini* the initial horizontal stress in the roof strata (MPa) in the direction perpendicular to entry development; *RSa* the weighted average field-scale strength of strata in the bolt anchorage zone (upper 0.6 m or 2 ft of fully grouted bolts) (MPa); *RSi* the weighted average field-scale strength of strata in the immediate roof (from roof line to start of bolt anchorage zone) (MPa); *RSc* the weighted average field-scale strength of strata in the cable anchorage zone (upper 1.2 m or 4 ft of cable bolts) (MPa); *SSc* a parameter representing standing support efficiency; and *RRb* and *RRc* the parameters representing the roof reinforcement provided by bolts and cable bolts, respectively.

The field-scale strength of the different roof strata units is derived from the uniaxial compressive strength (UCS) of the rock matrix and the rating of bedding strength according to the coal mine roof rating (CMRR) [18], as described by Esterhuizen et al. [19]. The reinforcement contribution of the fully grouted bolts (*RRb*) is calculated after Mark et al. [20].

$$RRb = (Nb \times Lb \times Cb)/(We \times Sb) \tag{6}$$

where *Nb* is the number of bolts per row; *Lb* the bolt length (m); *Cb* the bolt ultimate tensile capacity (kN); *We* the width of the entry (m); and *Sb* the spacing between rows of bolts (m).

The cable bolt contribution (*RRc*) is also calculated using Eq. (6), but replacing bolt dimensions and capacities with the appropriate values for the cable bolts.

The standing support contribution is determined from the work-rate of the standing supports. This allows the peak and post-peak yield capacity of the different standing supports to be accounted for. The work rate (*Sw*) is calculated as the average work (kN-m) per cm of compression when compressing a standing support by 0.30 m (12 in). Table 2 presents work rate of some typical

Table 2
Average work rate of some standing support types calculated over 0.30 m (12 in) of compression.

Support type	Work rate (kNm per cm)
3.15 mm (9pt) timber crib	3.39
0.60 m (24 in) engineered timber crib	6.78
0.25 m (10 in) engineered timber prop	2.71
0.76 m (30 in) pumpable crib	5.50
0.60 m (24 in) can type support	9.67

standing supports. The standing support contribution (*SSc*) is calculated as follows.

$$SSc = Sw/(Ns \times Ss) \tag{7}$$

where *Sw* is the average standing support work-rate over 0.30 m (12 in) of compression (kNm per cm); *Ns* the number of standing supports in each row (typically one or two); and *Ss* the center-to-center spacing between rows of standing supports (m).

3.2. Accounting for entry width and intersection effects on roof sag

Changes in the width of entries have a direct impact on roof deformation and stability. Intersections of two or more entries are generally less stable than single entries because larger roof spans are exposed, resulting in increased roof deformation and height of potential roof yield [21]. Fig. 2 illustrates the height of potential roof yield over entries and intersections in the gateroads of a typical longwall in the Pittsburgh coal bed, as predicted by a FLAC^{3D} model. Fig. 2 also shows the increased extent of failure in the roof of the belt entry at the longwall face corner caused by the longwall-induced horizontal and vertical stress changes. The results of initial modeling and analysis of intersections [22], combined with a review of model results such as those shown in Fig. 2, were used to formulate a procedure to adjust for the effect of entry and intersection width on roof stability.

For the RSR calculation, changes in entry width are accounted for by adjusting the roof sag calculated by Eq. (1) as follows.

$$s_w = 0.182 \times W \times s \tag{8}$$

where s_w is the width-adjusted roof sag (cm); *W* the excavation width in m; and *s* the roof sag (cm) calculated by Eq. (1). The constant value of 0.182 in Eq. (8) will result in an adjustment factor of 1.0 when the entry width is 4.8 m (16 ft), which was the base entry width used in the parametric studies.

The increased roof sag at intersections is estimated by setting *W* in Eq. (8) equal to 1.5 times the entry width for four-way intersections and 1.3 for three-way intersections. These increased excavation spans approximate the average diagonal spans at the intersections. These factors may be adjusted to assess the impact of increased intersection spans caused by coal sloughing at the pillar corners or poor mining practices.

3.3. Regression equation to estimate the height of detached roof

The yielded strata that may collapse if unsupported is referred to as the "detached roof" in this section and in further discussions.

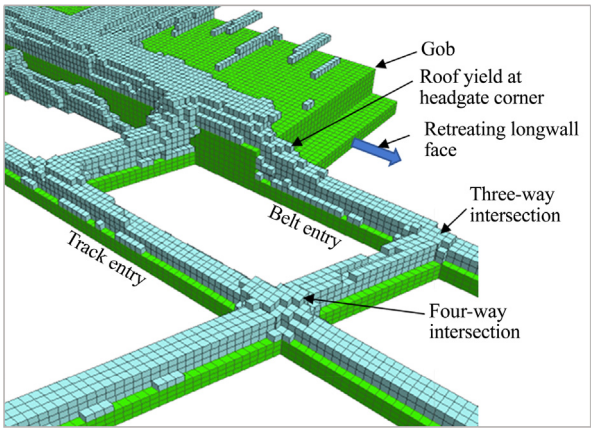

Fig. 2. Cutaway view of a three-dimensional FLAC^{3D} model of a retreating longwall showing roof yield above the entries and cross-cuts.

An equation to predict the height of detached roof was developed by considering the roof deformations predicted by the numerical models used in the parametric studies and statistics of the heights of reported roof falls in coal mines. The procedure that was followed was to determine the height of potentially detached roof in the entry models for each geologic scenario and loading condition evaluated. The height of detached roof was defined as the location where the roof sag exceeds 0.025 m (1 in). Roof sag is measured relative to a reference point 6.0 m (20 ft) above the roof line of the entry, which coincides with the length of extensometers used to measure roof deformation in the field studies.

The model results showed the height of detached roof is related to both the strength of the roof strata and the magnitude of roof sag measured at the entry roof line. The results also showed that the height of detached roof becomes limited as the yielded strata achieve a stable arch configuration over the excavation. The height of the stable arch in weak rock was found to be approximately equal to the width of the entry. In stronger rocks, a stable configuration may be achieved at a smaller height when a strong, non-yielding strata unit is encountered. The cumulative height of detached roof predicted by the numerical models agrees well with the cumulative height of several thousand roof falls in coal mines, reported to the Mine Safety and Health Administration (MSHA) [23], as shown in Fig. 3.

The regression equation for estimating the height of detached roof (*Y*) in meters is given below. The equation is based on least squares error fitting of the logistic curve to the detached height determined from the parametric study results.

$$Y = \frac{6.55 \times W/s_0}{1 + \exp[(-7.48/s_0)(s_w - 0.51 - 0.60 \times s_0)]} \tag{9}$$

where s_0 is the roof sag corresponding to the mid-height of the logistic curve (cm). The value of s_0 is estimated from Eq. (10).

$$s_0 = 4.0 \times 10^{-4} \times RS^2 + 0.112 \times RS + 8.873 \tag{10}$$

where *RS* is the weighted average field-scale roof strength in the bolted horizon (MPa) up to the top of the cable bolts. The field-scale roof strength is calculated as for Eq. (3). The average roof strength, therefore, affects both the ultimate height and shape of the curve. Note that for intersections, the value of s_w is already adjusted to account for the greater excavation width. To prevent double accounting for intersection effects, the original entry width *W* should be used in the calculation of the detached roof height.

3.4. Calculating roof support effectiveness

The effectiveness of roof support depends on its ability to prevent the detached roof strata from collapsing and is assessed by considering: (1) the ability of the bolts and cable bolts to accom-

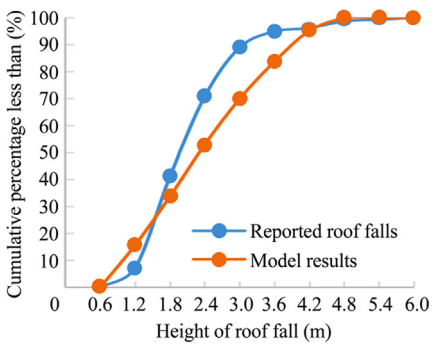

Fig. 3. Comparison of reportable roof fall heights in coal mines to numerical-model-predicted height of detached roof.

modate the longwall-induced roof deformations without failing, (2) the ability of the bolts and cable bolts to suspend the dead weight of the detached roof from the upper strata, and (3) the ability of the standing supports to resist the dead weight of the detached roof strata after being compressed by the roof sag and any potential floor heave.

The calculation of bolt load-carrying capacity considers the fact that bolt effectiveness is reduced when the height of detached roof starts to encroach on the anchorage zone of the fully grouted bolts, which is assumed to be the upper 0.6 m (2 ft) of the bolts. The load-carrying capacity of the bolts is assumed to linearly decrease to zero when the height of roof yield reaches 0.6 m (2 ft) above the top of the bolts. This assumption is partially justified by the fact that 69% of reported roof falls extend 0–0.6 m (0–2 ft) above the top of the bolted horizon [23].

For cable bolts, the impact of roof yield height on their load-carrying capacity is determined in the same manner as for bolts, described above. Two additional checks are made for cable bolts: (1) a check for the capacity of cable bolts to carry the weight of the detached roof strata, and (2) a check to determine if the roof sag exceeds the ultimate tensile strain limit of the cable bolts.

The contribution of standing supports is determined by comparing their support capacity to the dead-weight load of the detached roof rocks minus any weight borne by the roof reinforcement system. The support capacity of standing supports depends on the amount of compression of the supports by roof sag and floor heave. The regression equations presented above only predict the roof sag component. To account for the floor heave component, a constant relationship between roof sag and floor heave can be introduced. For example, it can be assumed that floor heave is a constant 50% of roof sag, based on observational evidence. Further work is required to provide a systematic method of estimating the occurrence and effects of floor heave based on geology and stress parameters.

3.5. Calculating the RSR

The RSR is calculated from the ratio of the load-carrying capacity of the support system relative to the dead weight of the detached roof. The RSR is expressed on a scale of 0 to 100 with larger values indicating increasing stability. When the roof load equals the support capacity, the RSR is 30 which equates to a safety factor (SF) of 1.0. RSR values of above 80 are expected to be highly stable, representing SFs greater than 2.5.

The RSR calculation is conducted by first determining whether any of the reinforcing elements may have failed due to elongation induced by roof yielding. Any failed supports obviously make no contribution to the support capacity. Next, the height of detached roof is compared to the bolt and cable-bolt lengths to determine whether roof yield may have reduced their support capacity. Finally, the dead weight of the detached roof is compared to the capacity of the reinforcing elements to determine their SF against overloading.

After considering the reinforcing elements, the capacity of the standing supports is evaluated. The standing support capacity depends on the amount of compression caused by roof sag and floor heave. The load-bearing capacity of the standing supports is determined from their load-deformation curve as tested in the NIOSH Mine Roof Simulator. The load-bearing capacity of the standing supports is then added to the capacity of the reinforcement system, which represents the overall load-bearing capacity of the supports.

The RSR is calculated from the ratio of the overall load-bearing capacity of the supports to the calculated dead weight of the detached roof strata as follows.

$$RSR = 90/(1 + 13.37\exp(-1.844 \times SF)) \quad (11)$$

$$SF = (Cb + Cc + Css)/Dy \quad (12)$$

where SF is the classic safety factor of the support system; Cb the capacity of fully grouted bolts (kN); Cc the capacity of the cable bolts (kN); Css the capacity of standing supports (kN); and Dy the weight of yielded roof strata (kN).

4. Case study example

The case study demonstrates how the procedure for assessing gateroad support performance was applied in a retrospective analysis of a roof fall at a three-way intersection in the headgate belt entry of a longwall mine operating in the Pittsburgh coal bed. The objective was to verify whether the procedure would successfully identify a potential roof fall in the headgate given the geology, support, and loading conditions.

The gateroads at the case study mine consisted of three entries each that were 4.8 m (16 ft) wide. The width of the gateroad was 65 m (215 ft) consisting of 30 m (100 ft) wide and 35 m (115 ft) wide pillars, with the larger pillar formed between the belt entry and the track entry. The depth of cover at the location of the roof fall was 243–274 m (800–900 ft). The pre-mining major horizontal stress in the strata was oriented at about 15° counterclockwise from the direction of headgate development and was, therefore, unfavorably oriented relative to the right-handed longwall setup [24].

4.1. Geotechnical information

The roof strata at this mine are typical of the Pittsburgh coal bed and consist of alternating coal riders and claystone beds in the immediate 0.9–1.8 m (3–6 ft) of the roof, overlain by moderate-strength shale grading to sandstone or limestone beds. At the location of the headgate roof fall, the roof geology was in a transition zone where the roof strata change from a sandstone-with-shale environment to a limestone environment with underlying claystone. Transition zones are known for their troublesome ground control [6,25] because of the presence of alternating layers of claystone, thinly bedded shale, and thinly bedded sandstone units. The claystone beds are problematic if they are present in the anchorage zone of the supports systems, and thinly bedded shale and sandstone units are susceptible to changes in the horizontal stress [26].

Fig. 4 illustrates the roof composition determined by borescope logging in the proximity of the headgate roof fall and at a NIOSH monitoring site in the gateroad of the same longwall panel. The roof at the location of the headgate fall contained several bands of claystone that resulted in poor anchorage of the support system, while the roof at the NIOSH monitoring site consisted of silty shale and sandstone, providing improved roof stability and anchorage for the roof reinforcement system.

In the absence of rock strength data from the local mining area, the rock strength was estimated based on testing results from mines that operate in the Pittsburgh coal bed. The mechanical properties of the strata used in the RSR assessment are shown in Table 3. Detailed roof-scoping observations of the sedimentary features [26] at both sites were used to assist in estimating the CMRR bedding ratings for the strata units in the roof.

4.2. Roof support system

The support system in the 4.8-m (16-ft) wide headgate belt entry consisted of two 2.7-m (9-ft) long, resin-assisted, torque-tension bolts installed on a T3-channel with a single 0.017-m

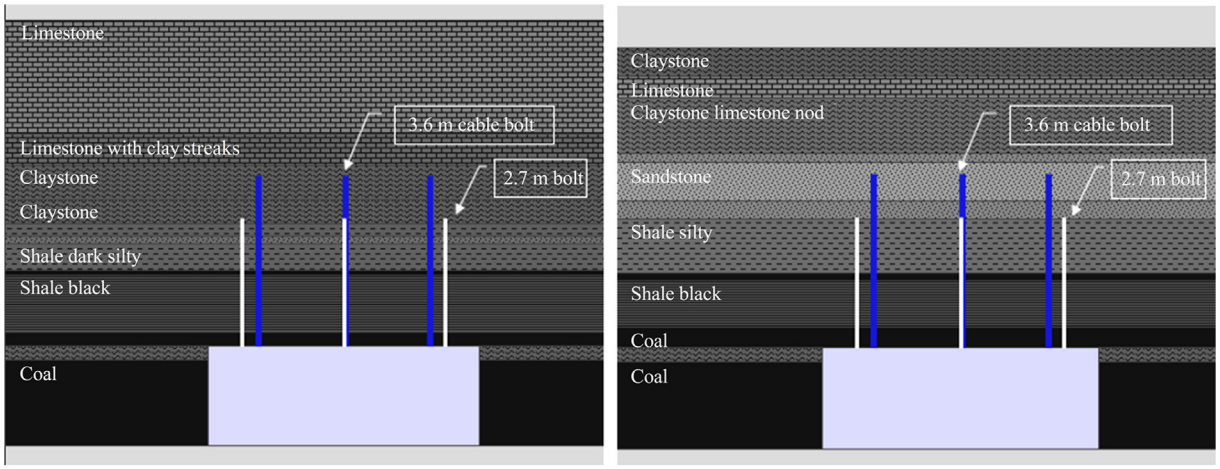

(a) At location of headgate roof fall (b) At location of NIOSH monitoring site

Fig. 4. Schematic illustration of roof geology, entry location, and belt entry roof reinforcement. Darker shading indicates lower rock strength.

Table 3
Strength properties of roof strata used for RSR assessment.

Rock type	UCS (MPa)	CMRR bedding rating
Coal	20.6	25
Claystone	17.9	20
Claystone with limestone nodules (LN)	24.1	30
Shale gray silty medium bedded (MB)	42.0	30
Shale gray thin bedded (TNB)	42.0	20
Shale dark thin bedded (TNB) with clay	31.0	20
Sandstone medium bedded (MB)	68.2	45
Sandstone thin bedded shale streaks (SHS)	48.2	25
Limestone with clay streaks (CS)	44.8	35
Limestone	60.6	45

(0.7-in) diameter cable-bolt in the center of the strap that is 3.6-m (12-ft) long. The support rows are 1.2 m (4 ft) apart. The track entry (middle entry) was supported by the three 2.7-m (9-ft), resin-assisted point-anchor combination bolts in rows 1.2 m (4 ft) apart with a 3.6-m (12-ft) cable bolt added every 2.4 m (8 ft) in the intersections. Standing support in the track entry was a single row of 1.4-mm (4-pt) timber cribs, and in the tailgate entry, two rows of 1.4-mm (4-pt) timber cribs were used at 2.4-m (8-ft) spacing. After the roof fall occurred in the headgate belt-entry, specialist contractors were brought in to inject resin grout to consolidate the roof. Two 4.8-m (16-ft) long, fully grouted (pumpable) cable bolts were additionally installed in rows 1.2 m (4 ft) apart between the rows of standard bolt supports. The additional support was able to successfully control the roof so that the longwall could advance through the transition zone after the roof fall had been cleaned-up.

4.3. Pre-mining stress

For the calculation of the RSR it was necessary to estimate the initial ground stress and stress changes induced by longwall mining. The initial ground stress was determined using the Mark and Gadde [27] procedure for estimating pre-mining horizontal stress in the eastern U.S. The longwall-induced horizontal and vertical stress changes were determined by a three-dimensional numerical model of a longwall with typical Pittsburgh seam geology that has the appropriate orientation of the panel relative to the major horizontal stress direction. Stress changes induced by the longwall were determined at locations 0.9 m (3 ft) above the roof line of the gateroad entries. These stress changes were used as inputs to the RSR calculation.

4.4. Monitoring ground response

NIOSH researchers installed ground monitoring instrumentation in the track entry beyond the transition zone to measure ground deformation and support response. The monitoring site was supported by the standard gateroad support system mentioned earlier. The site was monitored during the approach and passing of the first longwall, but longwall operations were abandoned before the second longwall mined-by the monitoring site. Details of the monitoring results were presented in Gearhart et al. [9]. Of interest here is that the average roof sag induced at the monitoring site by the passing of the first longwall panel was measured by the extensometers to be ranging from 0.027 to 0.035 m (1.1 to 1.4 in), with an average of 0.033 m (1.3 in). The monitoring site was located 35 m (115 ft) from the edge of the first longwall gob at a depth of cover between 259 and 304 m (850 and 1000 ft). The monitoring results were used to verify that Eq. (1) provides a reasonable estimate of the measured roof sag at this mine.

4.5. Calculation of RSRs

The above geotechnical data, support system, and field-monitored response were used as inputs to Eqs. (1) and (8) to estimate likely roof sag and the height of detached roof for various scenarios. Initially, the predicted roof sag at the NIOSH monitoring site in the track entry was calculated using the roof geology and strength data presented in Fig. 5 and Table 2 as inputs. The calculation showed longwall-induced roof sag of 0.017–0.027 m (0.7–1.1 in) induced by the passing of the first longwall for a depth of cover range of 259–304 m (850–1000 ft). This is considered to be reasonable compared to the measured longwall-induced sag of 0.033 m (1.3 in), given the degree of uncertainty in the input values used for the calculation.

The estimated roof sag and support performance for the belt entry and the three-way intersections were calculated next to see if the equations would successfully indicate the potential headgate roof fall. The depth of cover was set at 274 m (900 ft). The horizontal stress and vertical stress at the headgate corner were calculated to be 13.5 and 15.3 MPa (1963 and 2227 psi), respec-

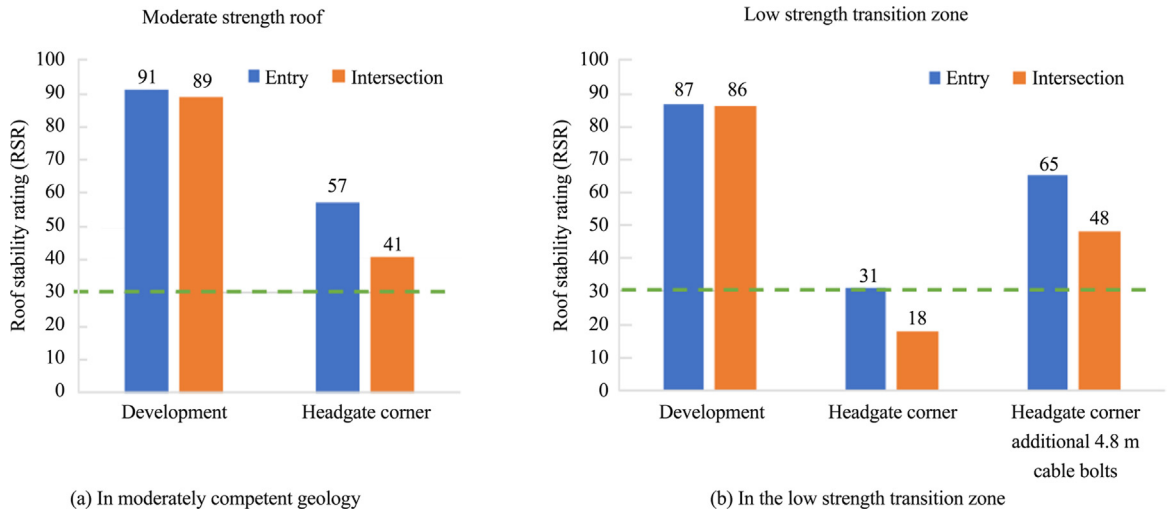

(a) In moderately competent geology (b) In the low strength transition zone

Fig. 5. Roof stability rating (RSR) for the longwall headgate belt entry. The impact of adding 4.8-m (16-ft) cable bolts on roof stability at the headgate corner in the weak transition zone is also shown.

tively, from the results of the 3D numerical model of the longwall mentioned earlier. The expected roof sag, support response, and RSR were calculated for both the transition-zone geology and the relatively stronger roof geology at the NIOSH monitoring site. The entry and intersection support systems employed at the mine were used as inputs. A final calculation was carried out to estimate the impact of the 4.8-m (16-ft) supplementary cable bolts that were installed during the recovery of the belt entry in the transition zone.

The RSR-calculated results for the headgate belt entry are summarized in Fig. 5. The dashed line at the RSR value of 30 indicates a critical stability condition at which the calculated support capacity equals the calculated roof load. This represents a SF of 1.0, which implies a 50% likelihood of failure of the support system according to the selected inputs and method of calculation. Fig. 5a shows that under the moderate strength roof conditions the RSR for development loading conditions is around 90 for both entries and intersections, which can be interpreted as highly adequate. At the headgate corner the RSR values drop to 57 and 41 for the entries and intersections, respectively. These RSR values resulted in adequate stability of the belt entry and intersections during normal operations.

The effect of the weaker transitional geology is shown in Fig. 5b. The RSR values under development conditions remain high at around 85, indicating stable conditions. This is because the roof sag is limited, and the 2.7-m (9-ft) long fully grouted bolts and 3.6-m (12-ft) long cable bolts can adequately control the roof. At the headgate corner, however, roof sag becomes excessive, and the height of roof yield is estimated to extend above the top of the 2.7-m (9-ft) bolts, while the dead weight of the detached roof strata loads the cable bolts to their limit. At this stage, the 2.7-m (9-ft) bolts are encapsulated within the yielding roof and are expected to provide reduced ground reinforcement. This limiting condition produces a SF against cable failure of 1.0 in the headgate entries. In the intersections, the height of roof yield is estimated to extend to 3.5 m (11.8 ft), which reduces the effectiveness of the cable bolts and also results in overloading of the cable bolts. The resulting RSR value of 18 falls well below the "critical" RSR of 30, indicating a high risk of roof collapse.

Finally, Fig. 5b also shows that the plan to install supplementary supports consisting of two 4.8-m (16-ft) cable bolts every 1.2 m (4 ft) as an emergency measure is predicted to restore the RSR value to 48 in the intersections and 65 in the entries. These cable bolts are successful because they extend beyond the estimated zone of roof yield and provide additional capacity to help carry the dead weight of the detached roof. The experience at the mine showed that the supplementary cable bolts did indeed help to control the roof and allow longwall operations to be re-established.

From this case study, it appears that for the local geology and estimated loading conditions, RSR values of above 40 are sufficient to achieve satisfactory headgate ground control at the mine.

5. Conclusions

A procedure to rate the stability of the roof of gateroad entries and intersections has been presented. The calculation procedure is based on field studies of gateroad support performance at longwall operations, numerical model analysis of the study sites, and additional parametric studies using the developed numerical models. The roof stability rating (RSR) describes the ability of the support system to control the yielded roof that would collapse if unsupported. The procedure to calculate the RSR makes use of regression equations that allow the roof sag and height of detached roof to be estimated, which are then used to determine the support response. The RSR compares the support load-bearing capacity to the dead weight of the detached roof. The RSR allows the impact of support systems and mine-layout alternatives on roof stability to be assessed during the planning stage of a longwall operation.

Several assumptions and simplifications were made to reduce the highly complex problem of excavation stability in yielded ground to a manageable scenario. The objective of the RSR is to allow persons who are responsible for longwall ground control to systematically compare their alternatives using a procedure that considers the geology, both horizontal and vertical stress changes, and both primary and standing support response to these changes.

The case study presented demonstrates that the RSR calculation is able to successfully discriminate between stable headgate conditions and conditions that resulted in a headgate roof fall. At the case study mine, RSR values of greater than 40 represented adequate headgate stability, while RSR values of 27 to 31 were associated with a headgate roof fall. The RSR of the remedial support that resulted in the successful continuation of mining in the transition zone was calculated to be 45 to 65. These RSR ranges are applicable for the case-study mine only and should not be considered to be representative of mines in other geologic settings.

The regression equations for calculating RSR are somewhat biased towards coal mine operations in the eastern U.S. The NIOSH Pittsburgh Mining Research Division is continuing to conduct

research related to entry stability in longwall mines, and as more field data and analysis results become available, the equations may be enhanced to incorporate the new information.

Disclaimer

The findings and conclusions in this report are those of the authors and do not necessarily represent the views of the National Institute for Occupational Safety and Health, Centers for Disease Control and Prevention. Mention of any company or product does not constitute endorsement by NIOSH.

References

[1] Sears MM, Esterhuizen GS, Tulu IB. Overview of current U.S. longwall gateroad support practices: An update. Mining, Metallurgy & Exploration 2019;36(6):1137–44.

[2] Mohamed KM, Murphy MM, Lawson HE, Klemetti T. Analysis of the current rib support practices and techniques in U.S. coal mines. Int J Mining Sci Technol 2016;26(1):77–87.

[3] Peng SS. Longwall mining. CRC Press; 2019.

[4] Lu J, Hasenfus G. Challenges of mining the first right-handed longwall panel in a new reserve block in Pittsburgh Seam. Int J Mining Sci Technol 2019;29(1):145–9.

[5] Barczak TM. Optimizing secondary roof support with the NIOSH Support Technology Optimization Program (STOP). In: Proceedings of the 19th international conference on ground control in mining. Morgantown, WV; 2000.p. 74–84

[6] Zhang P, Gearhart DF, Van Dyke M, Su DWH, Esterhuizen E, Tulu IB. Ground response to high horizontal stresses during longwall retreat and its implications for longwall headgate support. Int J Mining Sci Technol 2019;29(1):27–33.

[7] Batchler T. Analysis of the design and performance characteristics of pumpable roof supports. In: Proceedings of the 35th international conference on ground control in mining. Morgantown, WV; 2016.p.169–78

[8] Gearhart DF, Esterhuizen GS, Tulu IB. Changes in stress and displacement caused by longwall panel retreats. In: Proceedings of the 36th international conference on ground control in mining. Morgantown, WV; 2017.p.313–20

[9] Gearhart DF, Zhang P, Esterhuizen GS. Analysis of the effects of a passing longwall face on the roadway, pillars and standing supports. In: Proceedings of the 37th international conference on ground control in mining. Morgantown, WV; 2018.p.359–65

[10] Esterhuizen GS, Gearhart DF, Tulu IB. Analysis of monitored ground support and rock mass response in a longwall tailgate entry. Int J Mining Sci Technol 2018;28(1):43–51.

[11] Esterhuizen GS, Gearhart DF, Klemetti T, Dougherty H, Van Dyke M. Analysis of gateroad stability at two longwall mines based on field monitoring results and numerical model analysis. Int J Mining Sci Technol 2019;29(1):35–43.

[12] Tulu IB, Esterhuizen GS, Gearhart DF, Klemetti TM, Mohamed KM, Su DWH. Analysis of global and local stress changes in a longwall gateroad. In: Proceedings of the 36th international conference on ground control in mining. Morgantown, WV; 2017.p.100–10

[13] Klemetti TM, Van Dyke M, Compton CS, Tulu IB, Tuncay D, Wickline J. Longwall gateroad yield pillar response and model verification–a case study. In: Proceedings of the 53rd US rock mechanics/geomechanics symposium. Brooklyn: American Rock Mechanics Association; 2019

[14] Itasca Consulting Group. FLAC3D Fast Lagrangian Analysis of Continua in 3 Dimensions; 2014.

[15] Esterhuizen GS, Bajpayee TS, Murphy MM, Ellenberger JL. Evaluation of the strength reduction method for US coal mine entry stability analysis. In: Proceedings of the 7th international symposium on ground support in mining and underground construction. Australian Centre for Geomechanics; 2013. p.373–85.

[16] Tulu IB, Esterhuizen GS, Klemetti T, Murphy MM, Sumner J, Sloan M. A case study of multi-seam coal mine entry stability analysis with strength reduction method. Int J Mining Sci Technol 2016;26(2):193–8.

[17] Mirabile B, Westman E. Secondary support instrumentation in longwall ventilation entries. In: Proceedings of the 38th international conference on ground control in mining. Morgantown, WV: Society for Mining, Metallurgy and Exploration; 2019.p.350–6.

[18] Molinda GM, Mark C. Coal mine roof rating (CMRR): A practical rock mass classification for coal mines. IC 9387. Pittsburgh, PA: U.S. Department of the Interior, Bureau of Mines; 1994

[19] Esterhuizen GS, Bajpayee TS, Ellenberger JL, Murphy MM. Practical estimation of rock properties for modeling bedded coal mine strata using the Coal Mine Roof Rating. In: Proceedings of the 47th US rock mechanics/geomechanics symposium. american rock mechanics association; 2013.p.1634–47

[20] Mark C, Molinda GM, Dolinar DR. Analysis of roof bolt systems. In: Proceedings of the 20th international conference on ground control in mining. Morgantown, WV; 2000.p.218–25

[21] Molinda G, Mark C, Bauer E, Babich D, Pappas D. Factors influencing intersection stability in US coal mines. In: Proceedings of the 17th international conference on ground control in mining. Morgantown, WV; 1998.p.267–75

[22] Esterhuizen GS, Tulu IB, Klemetti T. Analysis of factors influencing coal mine intersection stability. In: Proceedings of the 48th US rock mechanics/geomechanics symposium. American Rock Mechanics Association; 2014.p.1968–77

[23] Bajpayee TS, Pappas DM, Ellenberger JL. Roof instability: What reportable noninjury roof falls in underground coal mines can tell us. Professional Safety 2014;59(3):57–62.

[24] Su DWH, Hasenfus GJ. Regional horizontal stress and its effect on longwall mining in the Northern Appalachian coal field. In: Proceedings of the 14th international conference on ground control in mining. Morgantown, WV; 1995

[25] Lu J, Van Dyke M, Su DWH, Hasenfus G. Transitional geology and its effects on development and longwall mining in Pittsburgh Seam. Int J Mining Sci Technol 2016;26(1):31–7.

[26] Van Dyke M, Klemetti T, Wickline J. Geologic data collection and assessment techniques in coal mining for ground control. In: Proceedings of the 38th international conference on ground control in mining. Morgantown, WV: Society for Mining, Metallurgy and Exploration; 2019.p.72–82

[27] Mark C, Gadde M. Global trends in coal mine horizontal stress measurements. In: Proceedings of the 27th international conference on ground control in mining. Morgantown, WV; 2008.p.319–31